

# The Photoelectron and Ultraviolet Spectra of Octamethylcyclododeca-1,3,7,9-tetrayne: a Weakly Antiaromatic Molecule

Cielo Santiago,<sup>1a</sup> K. N. Houk,\*<sup>1a,b</sup> Gary J. DeCicco,<sup>1c</sup> and Lawrence T. Scott<sup>1d</sup>

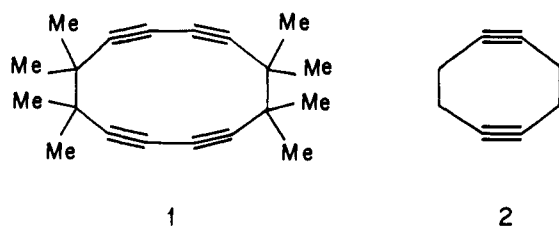
Contribution from the Departments of Chemistry, Louisiana State University, Baton Rouge, Louisiana 70803, University of California, Los Angeles, California 90024, and University of Nevada, Reno, Nevada 89557. Received June 24, 1977

**Abstract:** The photoelectron and ultraviolet absorption spectra of the title compound have been measured and interpreted with the aid of *ab initio* (STO-3G) and CNDO/S molecular orbital calculations. The photoelectron spectrum gives clear evidence of through-space interactions between the two conjugated diacetylene units situated essentially face-to-face across the 12-membered ring. The effects of bending at the acetylenic linkage and of through-bond interactions have been probed by calculations. These calculations indicate that the strong bending of the acetylenic units away from each other is due to cross-ring interactions. This molecule has both in-plane and out-of-plane antiaromatic eight-electron systems which promote bending. The ultraviolet spectrum is affected to a very small extent as compared to acyclic models in spite of the substantial cross-ring interaction. *Ab initio* calculations on 1,5-cyclooctadiyne suggest a different assignment for the first two bands in the photoelectron spectrum from the assignment made earlier on the basis of semiempirical calculations.

## Introduction

Octamethylcyclododeca-1,3,7,9-tetrayne (**1**) was recently synthesized in one of our laboratories.<sup>2</sup> This molecule provides an excellent opportunity to study the relative influence of (1) bending about the acetylenic linkage, (2) through-space interactions, and (3) through-bond interactions on the electronic structure of this and related molecules. **1** is formally a doubly bishomoantiaromatic molecule. That is, cross-ring overlap of the out-of-plane  $\pi$  orbitals produces an eight-electron system, and the molecule is expected to distort somewhat to relieve this interaction. Of even greater importance, the in-plane acetylenic  $\pi$  orbitals can overlap across the ring to produce an eight-electron " $\sigma$ -antiaromatic" molecule. As will be shown, substantial interactions of this system with the  $\sigma$  bridges can occur, but this only exacerbates the antiaromaticity of the  $\sigma$  system, producing a 12-electron antiaromatic system.

The x-ray crystallographic structures of **1**<sup>3</sup> and its more distorted, but less conjugated, analogue, 1,5-cyclooctadiyne (**2**)<sup>4</sup>, have been reported, as has the photoelectron (PE) spec-



trum of **2**.<sup>5</sup> By comparison of the spectra of these molecules, and by molecular orbital calculations, we have been able to determine that through-space interactions, rather than molecular distortions, in **1** cause a large split in the in-plane and out-of-plane  $\pi$  orbitals of this system (as revealed by PES) but lead to only a minor intensification of the  $\pi\pi^*$  transition of **1**.

## Photoelectron and Absorption Spectra of **1**

The photoelectron spectrum of **1** is shown in Figure 1.<sup>6</sup> There are two groups of peaks in the relatively low energy ionization region. The first group of bands, between 8 and 9.5 eV, shows two sharp prominent maxima at  $8.27 \pm 0.03$  and  $8.80 \pm 0.03$  eV. The *average* position of these two bands corresponds relatively closely to the position expected for the first ionization of di-*tert*-butyldiacetylene. Although the IPs of this compound have not been measured, they can be taken to be

approximately those of 5-decyne (8.67 and 11.1 eV).<sup>7</sup> The change of *n*-butyl to *tert*-butyl has essentially no effect on alkene IPs.<sup>8</sup>

Each of the first two maxima have tails which might be interpreted as vibrational structure ( $\sim 1800$  and  $500$   $\text{cm}^{-1}$  in the first band, and  $\sim 2100$  and  $500$   $\text{cm}^{-1}$  in the second, marked in Figure 1). The 1820 and 2100  $\text{cm}^{-1}$  vibrations correspond to acetylene  $\text{C}\equiv\text{C}$  stretching vibrations which are  $2250$   $\text{cm}^{-1}$  in the ground state (Raman spectrum).<sup>2</sup> However, each of these bands contains two ionizations, and assignment of IPs of 8.27, 8.50, 8.80, and 8.92 eV is more consistent with calculations (see below).

A third broad band, with no discernible vibrational structure, is observed at  $10.72 \pm 0.03$  eV in the PE spectrum of **1**. Finally, there is a sharp spike at 11.24 eV on the side of the  $\sigma$  onset. The separations between the first (8.27) and third (10.72) bands, and between the second (8.80) and fourth bands (11.24), are identical within experimental error, and the value of this separation, 2.45 eV, is only slightly smaller than that, 2.55 eV, found in 2,4-hexadiyne.<sup>7a</sup> The third and fourth bands are both in the region ( $\sim 11.1$  eV)<sup>8</sup> expected for the second IP of di-*tert*-butyldiacetylene. However, there is obviously a split in the various orbitals of **1** which correspond to the first and second doubly degenerate orbitals of di-*tert*-butyldiacetylene.

The ultraviolet spectrum also shows substantial deviations from that expected for an isolated diacetylene. In hexane, distinct maxima are observed at 237 ( $\epsilon$  687), 248 (750), and 264 nm (494), and there is a weak shoulder at 288 nm ( $\epsilon$  30). By comparison tetradeca-6,8-diyne, an acyclic model, has maxima at 227 ( $\epsilon$  360), 240 (350), and 253 nm ( $\epsilon$  200).<sup>10</sup> Thus, each band of **1** is shifted  $\sim 10$  nm bathochromically, but is of similar intensity, to those of an acyclic model, when the presence of two diacetylene units in **1** is taken into account.

There is substantial bending about the diacetylenic linkages in **1**, and, the  $\pi$  orbitals on opposite sides of the ring are sufficiently close to interact through space. Furthermore, through-bond interactions involving the saturated bridges are possible. In order to sort out the various interactions which give rise to the splittings of the various bands in the PES, we have carried out molecular orbital calculations described in the next section.

## Molecular Orbital Calculations on Model **1**

STO-3G calculations<sup>12</sup> were carried out on various models

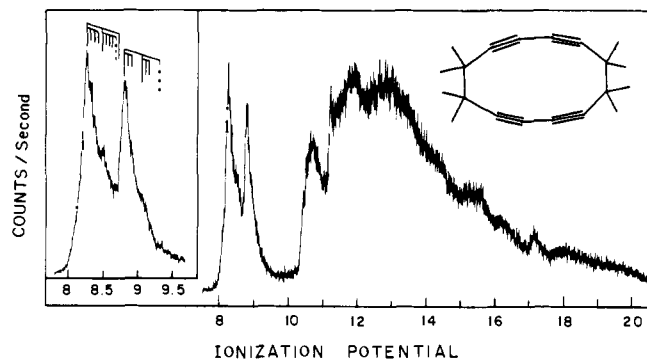


Figure 1. The photoelectron spectrum of tetrayne 1.

Table I. Orbital Energies of Models of 1 by STO-3G

Models	Orbital energies, eV			
	Lower energy pair		Higher energy pair	
	$\pi_{ip}$	$\pi_{op}$	$\pi_{ip}$	$\pi_{op}$
<b>A. Bending models</b>				
(1) Acetylene			-9.51	-9.51
(2) Acetylene, bent <sup>a</sup>			-9.46	-9.50
(3) Butadiyne	-8.31	-8.31	-11.8	-11.8
(4) Butadiyne, bent	-8.23	-8.29	-11.8	-11.8
(5) 2,4-Hexadiyne	-7.42	-7.42	-10.9	-10.9
(6) 2,4-Hexadiyne, bent	-7.34	-7.40	-10.9	-11.0
Model B <sup>b</sup>	-5.79	-6.97	-9.16	-10.5
	-8.44	-7.48	-12.0	-11.0
Model C	-6.84	-7.05	-9.84	-10.5
	-7.95	-7.65	-11.5	-11.3
Model D	-7.39	-7.21	-10.9	-10.7
	-7.45	-7.55	-10.9	-11.1
Model E (demethylated 1)	-6.57	-6.89	-9.97	-10.2
	-7.42	-7.30	-10.7	-10.6

<sup>a</sup> All sp angles bent 14° from linearity. <sup>b</sup> See Figures 2 and 3 for orbital symmetry classifications of models B, C, D, and E.

of 1 to assess the relative importance of bending acetylenic bonds and of through-space and through-bond interactions of  $\pi$  orbitals on the molecular orbitals. These calculations are summarized in Table I.

**A. Bending.** A number of investigations of the influence of bending upon the energies of the degenerate  $\pi$  orbitals of acetylenes have been reported.<sup>5,11</sup> Simultaneous cisoid bending of both HCC angles of acetylene causes essentially no change in the energy of the orbital perpendicular to the HCCH plane, but causes the in-plane  $\pi$  orbital to rise in energy, owing to antibonding admixture with the lower lying  $\sigma_{CC}(\sigma_{CH})$  orbital. The split in degeneracy for a bending angle of 13.4°, the distortion observed for each acetylenic linkage in 1, is only 0.1 eV by MINDO/2.<sup>11</sup> Since our calculations used the ab initio STO-3G method,<sup>12</sup> we repeated these calculations using this method.

Bending of both HCC angles in acetylene by 13.4° away from linearity causes a 0.04 eV split in degeneracy, while bending all four angles of 1,3-butadiyne by 13.4° splits the HOMO degeneracy by 0.05 eV, and the second pair of degenerate  $\pi$  orbitals by only 0.03 eV. In 2,4-hexadiyne, the corresponding values are 0.06 and 0.05 eV. Thus, bending alone is hardly able to explain the large splits observed in the photoelectron spectrum of 1.

**B. Through-Space Interactions.** Pure through-space interactions have been modeled by two 2,4-hexadiyne molecules aligned parallel, and separated by 2.695 Å. The orbitals which result from the calculation are shown in Figure 2, and the orbital energies are given in Table I.

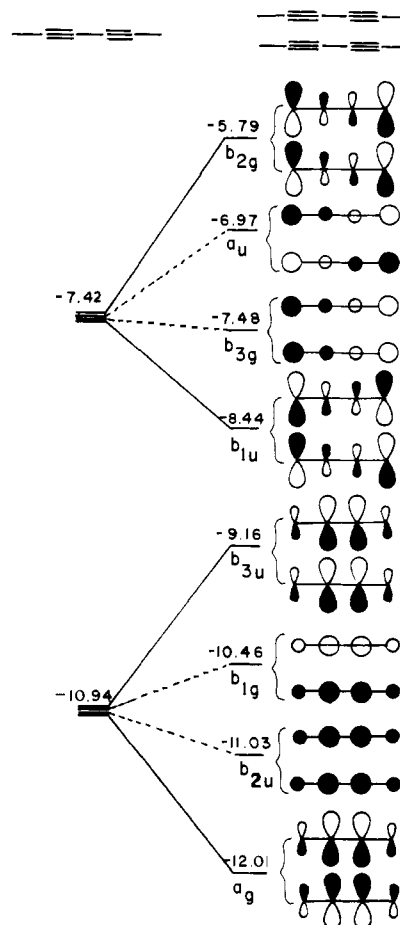


Figure 2. The molecular orbitals of a "supermolecule" consisting of two parallel 2,4-hexadiynes separated by 2.695 Å. ( $D_{2h}$  representations are given for z axis parallel to, and x axis bisecting, both diacetylene units.)

In the enforced  $D_{2h}$  geometry of the molecule, the four out-of-plane (op)  $\pi$  orbitals can be described as the bonding combination of the lowest energy diene  $\pi$  orbitals (of  $b_{2u}$  symmetry in  $D_{2h}$ ), the antibonding combination of the lowest energy diene op  $\pi$  orbitals ( $b_{1g}$ ), and, at higher energy, the bonding ( $b_{3g}$ ) and antibonding ( $a_u$ ) combinations of the op diacetylene highest occupied molecular orbitals (HOMOs). The in-plane (ip)  $\pi$  orbitals are, in order of increasing energy, the bonding and antibonding combination of lowest diene  $\pi$  orbitals ( $a_g$  and  $b_{3u}$ , respectively), and the bonding and antibonding combination of diacetylene ip HOMOs ( $b_{1u}$  and  $b_{2g}$ , respectively).

The resulting pattern of orbital energies is fully in accord with expectation for pure through-space interactions. The split in the degeneracy of the "in-plane  $\pi$ " orbitals is much greater than that of the out-of-plane  $\pi$  orbitals, in line with the ratio of overlap integrals for the two types of p orbitals, calculated for Slater orbitals at 2.695 Å ( $S(\sigma\sigma)/S(\pi\pi) = 0.061/0.011 = 5.5$ ).

**C. Through-Bond Interactions.** The influence of through-bond interactions was assessed by carrying out calculations on a crude model of the demethylated analogue of 1, cyclododeca-1,3,7,9-tetrayne, in which all cross-ring distances were held at 2.695 Å, but the methylenes were brought to within the bonding distance (1.602 Å) of 1. The orbital energies for this and other models are shown in Figure 3 and Table I.

This model has the  $D_{2h}$  symmetry of the "dimer". The splitting pattern of the energy levels is qualitatively similar to that of the dimer; the split in the degeneracy of the two pairs of ip  $\pi$  orbitals is larger than that of the op  $\pi$  orbitals. The split in the degeneracy of the two pairs of ip  $\pi$  orbitals of this bonded

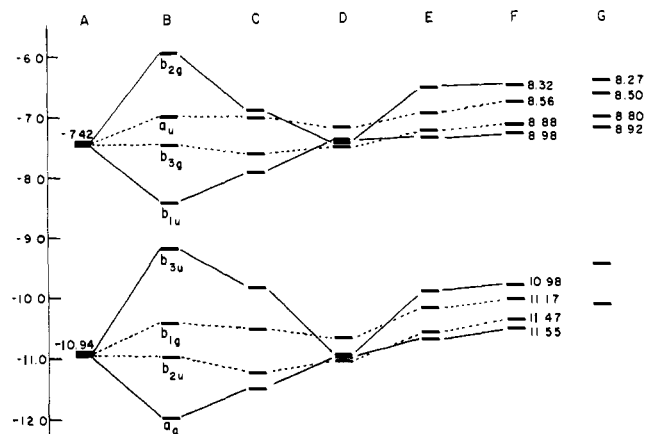


**Figure 3.** Correlations between STO-3G orbital energies of (A) two isolated 2,4-hexadiynes, (B) two linear 2,4-hexadiynes separated by 2.695 Å, (C) the planar ( $D_{2h}$ ) cyclododecatetrayne with linear diacetylene units, (D) the planar ( $D_{2h}$ ) cyclododecatetrayne with bent diacetylene units, (E) the  $C_{2h}$  cyclododecatetrayne with bent diacetylene units, (F) corrected Koopmans' ionization potentials of **1** (see text), (G) experimental ionization potentials of **1**.

model is smaller than that calculated for the nonbonded "dimer" owing to substantial interaction of the higher energy orbital of each pair ( $b_{2g}$  and  $b_{3u}$ ) with the  $\sigma^*$  C-C orbital and the lower energy orbital of each pair ( $b_{1u}$  and  $a_g$ ) with the  $\sigma$  CC orbital so that the orbitals of each pair are pushed closer together in energy.

**D. "Full Molecule" Calculations.** To compare the model calculations reported in the previous section to those on the actual geometry of **1**, we first performed a calculation on a demethylated model which was forced to be planar but otherwise had bond angles and lengths essentially identical with those found in the x-ray structure of **1**. This model increased the separation between the diyne units to 2.95 Å between  $C^{10}$  and  $C^1$  (2.70 Å in **1**) and 3.51 Å between  $C^9$  and  $C^2$  (3.24 Å in **1**). This geometry change drastically reduced  $\pi$  interactions to the point where both the higher energy pair and the lower energy pair remained essentially degenerate and had energies close to those calculated for 2,4-hexadiyne (-7.42 and -10.94 eV). Likewise, the energy separation in both the higher energy and the lower energy pairs of  $\pi$  orbitals is smaller than the previous model because of a diminished through-space interaction brought about by an increased separation of the diyne units.

Finally, we show the orbital energies calculated for the (nonplanar) x-ray structure of **1**, but with hydrogens substituted for methyls, on the far right of Figure 3. The molecule in the x-ray geometry of **1**<sup>3</sup> is shown in Figure 4. The molecule, **1**, consists of two bent diyne chains, one concave upwards and the other concave downwards. It has a center of inversion and the acetylene bond angles are bent from the usual linearity.

The top view of the molecule gives bond angles, bond lengths, and deviations (in Å) of the ring carbons from an imaginary plane. The side view of the molecule shows the relative positions of the atoms on the two buckled chains.

The molecular orbital shapes and relative energies for the actual molecular geometry are similar to those calculated for the planar model. Analytic geometry showed that the "in-plane" and "out-of-plane" orbitals were nearly perfectly determined by each bent diacetylene unit. The "in-plane" orbitals all lie in the  $C_1C_2C_3C_4$  plane on one half of the molecule and in  $C_7C_8C_9C_{10}$  plane on the other half. These orbitals are mainly  $\sigma$  but are not perfectly aligned. Similarly, the "out-of-plane" orbitals are perpendicular to these planes and are not quite perfectly  $\pi$  in character.

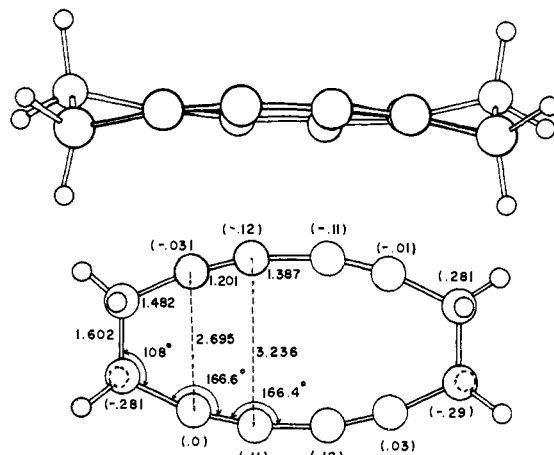


**Figure 4.** ORTEP plot of demethylated **1**. Large spheres are carbons, small spheres are hydrogens.

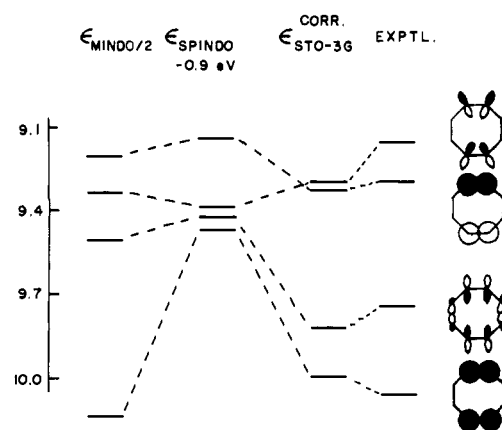


**Figure 5.** Calculated and experimental values of IPs of 1,5-cyclooctadiyne (MINDO/2, SPINDO, and experimental values for ref 5).

The orbital energy changes upon conversion of the planar model to the twisted one can be explained on this basis, as well as on the basis of the closer proximity of the two diacetylene units in the twisted geometry than in the planar one. That is,  $r_{1,10}$  and  $r_{2,9}$  decrease to 2.70 and 3.24 Å in the twisted molecule.

The orbital energy changes shown in Figure 3 are compatible with a substantial increase in the in-plane orbital interactions, which overrides the through-bond dominated split in the planar model. The out-of-plane interaction is increased to a smaller extent. The general upward drift in all of the orbital energies is, we believe, the result of small admixtures of various lower lying orbitals from the saturated bridges as the molecular symmetry is relaxed.

**Assignments of Photoelectron Spectra of **1** and 1,5-Cyclooctadiyne.** We felt it necessary to assess the reliability of STO-3G calculations in predicting ionization potentials in related systems, even though this type of calculation has an impressive record in the prediction of ionization potentials.<sup>14</sup> We have also carried out calculations on 1,5-cyclooctadiyne (**2**), a molecule similar to **1**, but lacking the conjugated diacetylene moieties. Heilbronner and co-workers carried out SPINDO and MINDO/2 calculations on this molecule and made photoelectron assignments essentially on this basis.<sup>5</sup> These assignments do not agree with those derived from STO-3G calculations shown in Figure 5. In the figure we plotted the experimental IPs of **2**, the corrected Koopmans' theorem IPs from STO-3G calculations, and Heilbronner's MINDO/2 and SPINDO IPs (0.9 eV was subtracted from all

**Table II.** STO-3G Calculated (Koopmans' Theorem) and Experimental  $\pi$  IPs of Acetylenes

Molecule	$-\epsilon(\text{STO-3G})$	$-\epsilon(\text{cor})^a$	Vertical IP
Acetylene	9.51	10.81	11.40
1,3-Butadiyne	8.31	9.87	10.17
	11.80	12.59	12.62
2,4-Hexadiyne	7.42	9.18	8.91
	10.94	11.92	11.46
1,5-Cyclooctadiyne ( <b>2</b> )	7.59	9.31	9.16
	7.62	9.33	9.30
	8.29	9.83	9.75
	8.48	10.00	10.07

<sup>a</sup> A least-squares regression analysis gives  $\text{IP} = 0.778 (-\epsilon^{\text{STO-3G}}) + 3.40$ , with a correlation coefficient of 0.969. This correction was used to calculate the values of  $-\epsilon(\text{cor})$  given in the second column.

the SPINDO IPs to give closer correspondence to experiment). The corrected STO-3G IPs are obtained using the least-squares correlation between the calculated and experimental IPs given in Table II. There appears to be a better correspondence between the STO-3G predictions and experiment than is observed for the semiempirical calculations. Furthermore, the STO-3G results are amenable to a relatively simple interpretation: the in-plane orbitals are raised very slightly relative to the out-of-plane by bending; secondly, through-space interactions cause a similar split in the degeneracy of in-plane and out-of-plane orbitals; finally, the bonding in-plane combination is raised by "through-bond" interactions, i.e., hyperconjugative interaction with a relatively high lying  $\sigma$  orbital of the saturated bridge. SPINDO and MINDO/2 apparently significantly underestimate the through-space interaction between the in-plane orbitals. In retrospect, this is not surprising since Gordon and co-workers found that interactions at distances beyond normal bonding separations are underestimated.<sup>15</sup> However, as Heilbronner has noted,<sup>5</sup> the final orbital energies are a complex mix of large through-space and through-bond interactions.

Because of the success of STO-3G calculations in providing reasonable interpretations of IPs of **2** and simpler acetylenes, we adopt the STO-3G assignments for **1**. However, it is necessary to make some estimate of the effect of methylation. We have done this crudely in the following way: "conversion" of diethyldiacetylene to di-*n*-butyldiacetylene causes a 0.10 eV decrease in IP;<sup>7</sup> if four carbons are added at each terminus of the diacetylene, we might expect approximately an 0.2 eV lowering of each IP of **1**. The predicted values [ $-\epsilon(\text{cor}) - 0.2$  eV] are plotted in Figure 3, along with the experimental values. As mentioned earlier, there is some doubt about whether certain maxima in the first band are due to separate ionizations or to vibrational structure. In light of the agreement between the first four calculated and experimental IPs, the former interpretation is preferred.

In this analysis, we have assumed that the conformation of **1** in the gas phase is the same as that in the crystal. However, the molecule is probably relatively flexible, and some of the lack of resolution in the PE spectrum may arise from conformational flexibility. A solution barrier to inversion of ca. 6 kcal/mol was determined by low-temperature NMR analysis.

The STO-3G calculations predict that the planar structure with bent diacetylene units is 15 kcal/mol more stable than the x-ray geometry. However, our calculations were performed without methyls, which are expected to force noncoplanarity due to methyl-methyl eclipsing repulsions in the planar species. It is amusing to note that a slight twisting of the molecule away from the x-ray geometry towards the planar would render the first and second IPs accidentally degenerate, as can be seen from Figure 3. Similarly, each pair of higher energy IPs would

be degenerate at a somewhat less twisted geometry. These accidental degeneracies would probably fit better with the experimental spectrum.

**Is **1** Antiaromatic?** As we have noted before, the interaction of the eight out-of-plane  $\pi$  electrons should be destabilizing, and the interaction of the eight in-plane  $\pi$  electrons, either through space or through bonds (which produces a 12-electron antiaromatic system), can be even more destabilizing. The photoelectron spectrum does not directly reveal antiaromaticity, but the large interactions between occupied orbitals should be destabilizing. The molecule would be expected to distort in such a fashion to minimize these interactions.

Calculations indicate that much of the molecular distortion present in **1** may be due to these antiaromatic interactions. The model referred to earlier in which the diacetylene units were held linear, but the remainder of the cyclododecatetrayne molecule was fixed near the x-ray geometry of **1** ( $\angle\text{C}_4\text{C}_5\text{C}_6 = 158.4^\circ$ ), was 11 kcal/mol less stable than the planar fully distorted molecule with  $\angle\text{C}_1\text{C}_2\text{C}_3 = 166.4^\circ$  and  $\angle\text{C}_2\text{C}_3\text{C}_4 = 166.6^\circ$ , according to STO-3G calculations. By comparison, 2,4-hexadiyne distorted to a geometry mimicking that of **1** (all  $\angle\text{CCC}'s \approx 166^\circ$ ) was only 0.4 kcal/mol more stable than a model with  $\angle\text{C}_1\text{C}_2\text{C}_3 = 158.4^\circ$ ,  $\angle\text{C}_2\text{C}_3\text{C}_4 = 180^\circ$ . Thus, the antiaromaticity induced by cross-ring interaction provides a substantial driving force for distortion of the molecule, making a simultaneous  $8^\circ$  bending of all of the terminal sp angles and  $14^\circ$  bending of all of the internal sp angles 10 kcal/mol more exothermic than in the acyclic case. The substantial bending in **1**, and the long  $\text{C}_5\text{C}_6$  and  $\text{C}_{11}\text{C}_{12}$  single bonds may be manifestations of the moderate antiaromaticity in **1**.

**The Ultraviolet Spectrum of **1**.** As noted in the Introduction, the UV spectrum of **1** is shifted by about 10 nm to longer wavelength than the positions observed for the acyclic models, or for molecules such as **1**, but in which the diacetylene units are connected by chains containing four or five methylene units. Sondheimer and co-workers found that the positions of the absorptions of cyclotetradeca-1,3,8,10-tetrayne are 239 ( $\epsilon$  600), 247 ( $\epsilon$  590), and 263 nm ( $\epsilon$  370).<sup>10</sup> **1** has almost identical maxima of  $\sim 10\%$  greater intensity. A similar sudden bathochromic shift and small decrease in intensity is observed in cyclophanes with one or both bridges containing three or fewer carbons. This has been attributed to both a puckering of the benzene rings and to cross-ring interaction.

Actually the differences in the UV spectra of **1** and acyclic analogues are surprisingly small as compared to the large splits in orbital degeneracies observed in the PE spectrum, so perhaps a better question to pose might be: why is the UV of **1** so similar to that of an acyclic analogue, in spite of the significant transannular interactions which are evident in the PE spectrum?

In order to answer this question in somewhat more than qualitative detail, we have carried out CNDO/S<sup>16</sup> calculations on **1** and acyclic models. In 2,4-hexadiyne, as in nonconjugated acetylenes, the lowest singlet state is forbidden and degenerate, involving configurations where one electron has been transferred from the "in-plane" HOMO to the "out-of-plane" LUMO, and vice versa. This transition is a  $\pi \rightarrow \pi^*$  transition, where the prime indicates an orbital perpendicular to the  $\pi^*$  orbital. The allowed  $\pi \rightarrow \pi^*$  transitions are at higher energy in the vacuum UV. The CNDO/S calculations (which predict the same order of orbital energies for **1** as are predicted by STO-3G) indicate that bending all the CCC angles of 2,4-hexadiyne by  $14^\circ$  should cause a lifting of the lowest singlet state degeneracy, a result mainly of the relatively substantial split of the LUMOs. The lowest singlet state becomes essentially pure HOMO (out-of-plane)  $\rightarrow$  LUMO (in-plane), and this is predicted to be at 0.13 eV lower energy than the SHOMO (in-plane)  $\rightarrow$  SLUMO (out-of-plane) transition. For comparison, in the linear compound, these two configurations

contribute equally to both of the degenerate lowest singlet states.

Amusingly, combining these two bent units in a planar model for **1** nearly restores the degeneracy (now fourfold) of the lowest singlet state, and causes essentially no change in the energy of the lowest singlet from that in the bent diyne model, in spite of the fact that there is a 0.18 eV difference in energy between the HOMO and SHOMO, according to CNDO/S. The lowest singlet state is composed of two-thirds of the configuration involving transfer of an electron from the HOMO (antibonding combination of in-plane diyne HOMOs) to the third vacant orbital (antibonding combination of out-of-plane diyne LUMOs) and one-third of the configuration involving transfer of an electron from the fourth occupied MO (bonding combination of in-plane diyne HOMOs) to the SLUMO (bonding combination of out-of-plane diyne LUMOs). The second, third, and fourth excited singlets are similar, involving a combination of transitions from in-plane occupied to out-of-plane vacant orbitals, or out-of-plane occupied to in-plane vacant orbitals. The multiconfiguration nature of the excited states results in clever masking by the molecule of the significant orbital energy changes which occur.

Thus, ultraviolet absorption spectroscopy appears not to be a particularly sensitive probe of the type of electronic interactions studied here, whereas photoelectron spectroscopy reveals significant interactions.

**Acknowledgment.** We wish to thank the National Science Foundation for financial support of this research. We also wish to thank Frank Fronczek for assistance with the calculations,

and Michael Squillacote for low-temperature NMR measurements.

## References and Notes

- (1) (a) Louisiana State University. (b) Camille and Henry Dreyfus Teacher-Scholar Grant Recipient, 1972-1977; Alfred P. Sloan Foundation Research Fellow, 1975-1977. (c) University of California. (d) University of Nevada.
- (2) L. T. Scott and G. J. DeCicco, *Tetrahedron Lett.*, 2663 (1976).
- (3) R. Weiss, Ph.D. Dissertation, University of California, Los Angeles, Calif., 1976.
- (4) E. Kloster-Jensen and J. Wirz, *Helv. Chim. Acta*, **58**, 162 (1975).
- (5) G. Bieri, E. Heilbronner, E. Kloster-Jensen, A. Schmelzer, and J. Wirz, *Helv. Chim. Acta*, **57**, 1265 (1974).
- (6) The photoelectron spectrum was recorded on a Perkin-Elmer PS-18 photoelectron spectrometer with an He(I) source, using xenon and argon as calibration standards.
- (7) (a) F. Brogli, E. Heilbronner, V. Hornung, and E. Kloster-Jensen, *Helv. Chim. Acta*, **56**, 2171 (1973); (b) E. Heilbronner, T. B. Jones, and J. P. Maier, *ibid.*, **60**, 1697 (1977).
- (8) P. Masclat, D. Grosjean, G. Mouvier, and J. Dubois, *J. Electron Spectrosc. Relat. Phenom.*, **2**, 225 (1973).
- (9) P. Carlier, J. E. Dubois, P. Masclat, and G. Mouvier, *J. Electron Spectrosc. Relat. Phenom.*, **7**, 55 (1975), report a value of 9.05 eV for this IP.
- (10) F. Sondheimer, Y. Amiel, and R. Wolovsky, *J. Am. Chem. Soc.*, **79**, 6263 (1957).
- (11) H. Schmidt, A. Schweig, and A. Krebs, *Tetrahedron Lett.*, 1471 (1974).
- (12) STO-3G calculations used Gaussian 70, QCPE No. 236, by W. J. Hehre, W. A. Lathan, R. Ditchfield, M. D. Newton, and J. A. Pople, and the STO-3G basis set described by W. J. Hehre, R. F. Stewart, and J. A. Pople, *J. Chem. Phys.*, **51**, 2657 (1969).
- (13) D. J. Cram, N. L. Allinger, and H. Steinberg, *J. Am. Chem. Soc.*, **76**, 6132 (1954).
- (14) P. D. Mollere and K. N. Houk, *J. Am. Chem. Soc.*, **99**, 3226 (1977); E. J. McAlduff and K. N. Houk, *Can. J. Chem.*, **55**, 318 (1977); L. N. Domelsmith, K. N. Houk, J. W. Timberlake, and S. Szilagyi, *Chem. Phys. Lett.*, **48**, 471 (1977); L. N. Domelsmith, K. N. Houk, R. A. Snow, and L. A. Paquette, *J. Am. Chem. Soc.*, in press.
- (15) M. D. Gordon, T. Fukunaga, and H. E. Simmons, *J. Am. Chem. Soc.*, **98**, 8401 (1976).
- (16) J. Del. Bene and H. H. Jaffé, *J. Chem. Phys.*, **48**, 1807, 4050 (1968); **49**, 1221 (1968); **50**, 563 (1969).

## Proton Magnetic Resonance and Conformational Energy Calculations of Repeat Peptides of Tropoelastin. The Hexapeptide

Dan W. Urry,\* Md. Abu Khaled, V. Renugopalakrishnan, and Rao S. Rapaka

*Contribution from the Laboratory of Molecular Biophysics and the Cardiovascular Research and Training Center, University of Alabama Medical Center, Birmingham, Alabama 35294. Received May 13, 1977*

**Abstract:** Detailed proton magnetic resonance data, obtained in chloroform-dimethyl sulfoxide solutions, are reported and utilized to derive a static approximation to the conformation of the repeat hexapeptide of tropoelastin, HCO-L-Ala<sub>1</sub>-L-Pro<sub>2</sub>-Gly<sub>3</sub>-L-Val<sub>4</sub>-Gly<sub>5</sub>-L-Val<sub>6</sub>-OMe. The experimental information includes data and analyses of all of the  $\alpha$ CH-NH and the valyl  $\alpha$ CH- $\beta$ CH coupling constants allowing estimates of five  $\phi$  and two  $\chi$  torsion angles, of temperature dependence of peptide NH chemical shift providing information on secondary structure, and of nuclear Overhauser enhancement data allowing estimates of two  $\psi$  torsion angles. The secondary structure and torsion angle data are self-consistent giving rise to a satisfactory static model. Conformational energy calculations in vacuo are also reported for the hexapeptide which describe two conformational states one of which compares favorably with the experimentally derived conformation. Adding to the static model a Val<sub>6,i-1</sub> residue preceding the hexapeptide and fixing the  $\phi$  and  $\psi$  angles of both Val<sub>6</sub> residues at the theoretically derived values allows formation of a 23-atom hydrogen-bonded ring which had previously been deduced in solution for the polyhexapeptide.

### Introduction

Tropoelastin, the precursor protein of the biological elastin fiber, has been shown to contain three repeating peptide sequences: a tetrapeptide (L-Val<sub>1</sub>-L-Pro<sub>2</sub>-Gly<sub>3</sub>-Gly<sub>4</sub>)<sub>n</sub>, a pentapeptide (L-Val<sub>1</sub>-L-Pro<sub>2</sub>-Gly<sub>3</sub>-L-Val<sub>4</sub>-Gly<sub>5</sub>)<sub>n</sub>, and a hexapeptide (L-Ala<sub>1</sub>-L-Pro<sub>2</sub>-Gly<sub>3</sub>-L-Val<sub>4</sub>-Gly<sub>5</sub>-L-Val<sub>6</sub>)<sub>n</sub>.<sup>1,2</sup> Previous spectroscopic studies on the hexapeptide of tropoelastin,

using primarily the methods of proton and carbon-13 magnetic resonance, have resulted in proposed intramolecular hydrogen bonds.<sup>3,4</sup> These hydrogen bonds are Ala<sub>1</sub> C-O...HN Val<sub>4</sub>, Gly<sub>3</sub> NH...O-C Gly<sub>5</sub>, and a weaker interaction, Gly<sub>3</sub> C-O...HN Gly<sub>5</sub>. This description of preferred secondary structure falls short of a desired description which would include specification of all of the  $\alpha$ CH-NH ( $\phi$ ), the  $\alpha$ CH-C' ( $\psi$ ), and the  $\alpha$ CH-